# Hydration dependent studies of highly aligned multilayer lipid membranes by neutron scattering

Marcus Trapp,[1,2] Thomas Gutberlet,[3] Fanni Juranyi,[4] Tobias Unruh,[5] Bruno Demé,[2] Moeava Tehei,[6] and Judith Peters[1,2,7,a)]

[1]*Institut de Biologie Structurale J.-P. Ebel, UMR 5075, CNRS-CEA-UJF, 41 rue Jules Horowitz, 38027 Grenoble, France*
[2]*TOF/HR Group, Institut Laue Langevin (ILL), 6 Avenue J. Horowitz, BP 156, F-38042 Grenoble Cedex 9, France*
[3]*Jülich Centre for Neutron Science, TU Munich, Lichtenbergstr. 1, 85747 Garching, Germany*
[4]*Laboratory for Neutron Scattering, ETH Zürich and Paul Scherrer Institut, 5232 Villigen PSI, Switzerland*
[5]*Physik Department E13 and Forschungsneutronenquelle Heinz Maier-Leibnitz FRM II, Technische Universität München, Lichtenbergstr. 1, 85747 Garching, Germany*
[6]*Australian Institute of Nuclear Science and Engineering (AINSE), Menai 2234, New South Wales, Australia and School of Chemistry and Centre for Medical Bioscience, University of Wollongong, Wollongong, New South Wales 2522, Australia*
[7]*Université Joseph Fourier, F-38041 Grenoble Cédex 9, France*

(Received 26 April 2010; accepted 12 September 2010; published online 25 October 2010)

We investigated molecular motions on a picosecond timescale of 1,2-dimyristoyl-*sn*-glycero-3-phosphocholine (DMPC) model membranes as a function of hydration by using elastic and quasielastic neutron scattering. Two different hydrations corresponding to approximately nine and twelve water molecules per lipid were studied, the latter being the fully hydrated state. In our study, we focused on head group motions by using chain deuterated lipids. Information on in-plane and out-of-plane motions could be extracted by using solid supported DMPC multilayers. Our studies confirm and complete former investigations by König *et al.* [J. Phys. II (France) **2**, 1589 (1992)] and Rheinstädter *et al.* [Phys. Rev. Lett. **101**, 248106 (2008)] who described the dynamics of lipid membranes, but did not explore the influence of hydration on the head group dynamics as presented here. From the elastic data, a clear shift of the main phase transition from the $P_\beta$ ripple phase to the $L_\alpha$ liquid phase was observed. Decreasing water content moves the transition temperature to higher temperatures. The quasielastic data permit a closer investigation of the different types of head group motion of the two samples. Two different models are needed to fit the elastic incoherent structure factor and corresponding radii were calculated. The presented data show the strong influence hydration has on the head group mobility of DMPC. © *2010 American Institute of Physics*. [doi:10.1063/1.3495973]

## I. INTRODUCTION

Native biological systems are always found in aqueous environments. Therefore, it is not surprising that the dynamics of such systems is influenced by the hydration level, as it has been confirmed by several neutron scattering studies[1–6] and molecular dynamics simulations.[7–9] The dynamical transition for proteins appears around 200 K. It marks the crossover from a regime in which only vibrational motions of the atoms are observed to a regime where anharmonic motions emerge. Below a certain level of hydration (typically 0.2–0.4 g water/g protein) corresponding to one complete water layer bound to the protein surface, the protein shows no dynamical transition and as a consequence does not become active.[4]

In the case of membranes, a transition due to the structural transition into the liquid-crystalline $L_\alpha$ phase is observed. Depending on the chain length and the degree of hydration of the lipid, it occurs around room temperature or even higher temperatures.[10] In contrast to proteins where the hydration of individual amino acids allows local motions of the protein, in phospholipid bilayers, only the hydration of the hydrophilic head group triggers the dynamic response of the hydration shielded hydrophobic acyl chains due to the increased surface available with increased hydration. For membranes, a shift of the main phase transition to higher temperatures with decreasing water content is already known for quite some time.[11] In recent years, neutron scattering studies of membrane dynamics focused on highly hydrated samples,[12–15] but only a few of these studies took hydration effects explicitly into consideration, e.g., König *et al.*[14]

In this work, we investigated the hydration influence on the dynamics of model membranes by quasielastic neutron scattering (QENS) and elastic incoherent neutron scattering. Model membrane systems such as 1,2-dimyristoyl-*sn*-glycero-3-phosphocholine (DMPC) show a similar thermodynamical behavior as real cell membranes[16] and are therefore often used to mimic their more complex natural counterparts.

Dynamics in such lipid systems span over a large range

a)Author to whom correspondence should be addressed. Electronic mail: peters@ill.fr.

 

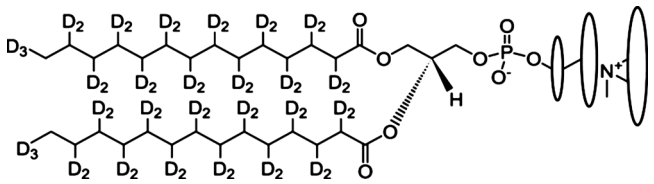

FIG. 1. Schematic view of DMPC-d54. According to the Carpentier model, three different radii are sketched in the choline head group.

in time and space, and have been investigated not only by neutron scattering,[12–14,17,18] but also by nuclear magnetic resonance,[19,20] inelastic x-ray scattering,[21] dielectric spectroscopy,[22] differential scanning calorimetry,[23] dynamic light scattering,[24] single particle tracking,[25] and other methods. To mimic membrane behavior in biological systems the fully hydrated state is the one of interest because this resembles physiological conditions. On the other hand, also the dried state is of interest, e.g., for food science.[26]

The knowledge of the dynamical behavior of these model systems as a function of hydration is then crucial to better understand the parameters necessary for the functioning of biological membranes and what precisely are their effects.[27]

## II. SAMPLE PREPARATION AND CHARACTERIZATION

In neutron scattering, deuterated samples allow to take advantage of the great difference in the incoherent scattering cross sections of hydrogen [$\sigma_{inc}=80.26$ b (Ref. 28)] and its isotope deuterium ($\sigma_{inc}=2.05$ b), whereas the coherent scattering cross sections are of the same order of magnitude [$\sigma_{coh}(H)=1.76$ b and $\sigma_{coh}(D)=5.59$ b, all values are given for thermal neutron with an incident wavelength of about 1.8 Å]. So selective deuteration can be used to change the contrast between different parts of the sample. This method is especially useful for biological samples which contain a high amount of homogeneously distributed hydrogen atoms. In phospholipid model membranes, the incoherent scattering cross section is drastically decreased by deuterating the alkyl-chains of the lipids. For completely protonated DMPC, the contribution to the incoherent scattering of the head group accounts for 25% of the total incoherent scattering. However, for the chain deuterated lipid used in our experiments, 73% of the total (incoherent+coherent) scattering cross section stems from the head group. The ratio is even more striking considering only the incoherent cross section, here 93% of the scattering originates from the head group. In the gel phase, the chains are arranged in a regular manner at a characteristic distance. This ordering gives rise to the coherent scattering originating from a quasi-Bragg peak around 1.48 $Å^{-1}$, the so called "chain correlation peak," corresponding to a distance of about 4.2 Å. In the liquid phase, the motion of the lipid chains prevents their ordering, and therefore the appearance of the correlation peak.

For the experiments described in the paper, we used chain deuterated DMPC-d54 (including the methyl groups at the end of the alkyl chains, see Fig. 1). The lipids were purchased from Avanti Polar Lipids (Alabaster, AL, USA) and used without any further purification (deuteration of ≥98%). The DMPC powder was dissolved in a 3:1 chloroform-trifluoroethanol mixture following a protocol described by Ding and co-workers.[29] The dissolution was kept at −20 °C overnight. To be able to probe the in- and out-of-plane motions of the lipids in the membranes, oriented samples have to be used. Such oriented samples have to be prepared on very smooth surfaces such as silicon wafers. The wafers were purchased from Siltronix (Archamps, France) with a thickness of 380(25) $\mu m$ and Si (111) orientation. Each Si-wafer was cut to a size of about 30 mm × 40 mm to fit the dimensions of the flat aluminum sample container used for the experiments. To avoid chemical interactions between the holder and the sample, the cells are coated with a layer of 3 $\mu m$ nickel and 0.5 $\mu m$ gold. About 30 mg of lipid solution was sprayed onto a single wafer. Using this method, bilayer stacks parallel to the wafer surface are assembled. Two samples with different hydration levels were prepared. After the deposition, the wafers were dried over silica gel for 2 days in a desiccator. One sample was rehydrated from pure $D_2O$ at 40 °C to achieve a fully hydrated sample (corresponding to about 12 water molecules per lipid and more[30]). The other one was rehydrated from a saturated salt solution to get reduced water content compared to the fully hydrated sample ($D_2O$+NaCl at 40 °C resulting in a relative humidity of 75%, about 9 water molecules per lipid). For each sample, six wafers were stacked together after rehydration to achieve a total amount of about 200 mg lipid per sample. A flat cover was used to close the sample cells. The total sample thickness of the six wafers (total thickness of 2.3 mm) and deposited DMPC was 3 mm. With typical values of about 90% for the sample transmission, this amount of sample is needed to achieve sufficiently high statistics in a reasonable measuring time. The weight of both samples was monitored before and after the experiments and no change was observed.

The level of hydration and the mosaicity of the samples were characterized by neutron diffraction prior to both the quasielastic and elastic experiments. The corresponding diffraction data obtained at D16 (Ref. 31) of the Institut Laue Langevin (ILL), Grenoble, France, are shown in the supplements to this paper.[32] This allows evaluating the bilayer repeat distance for each sample and by this means the relative humidity.[33] For the sample hydrated from pure $D_2O$, which will be referred to as the "higher hydrated sample" in the following, the diffraction data yield a repeat distance of 62.5 Å. The mosaic spread was extracted from fitting a Lorentzian curve to the experimental data to be 0.22(2)° [full width at half maximum (FWHM)]. The sample hydrated from $D_2O$+NaCl showed a d-spacing of 54.9 Å and a mosaicity of 0.25(2)° (data not shown here). It will be referred to as "less hydrated sample."

## III. EXPERIMENT

### A. Elastic experiments at IN13

Elastic experiments were performed at the Collaborative Research Group (CRG) thermal neutron backscattering spectrometer IN13 at ILL, Grenoble. The incident wavelength was $\lambda=2.23$ Å with an incident neutron energy of about 16 meV. This setup results in a uniquely wide range of mo-

mentum transfer $Q(0.2\ \text{Å}^{-1} < Q < 4.9\ \text{Å}^{-1})$. The elastic energy resolution was 8 $\mu$eV. A detailed description of the instrument and selected applications in the field of biophysics can be found in Natali *et al.*[34] Transmission for both samples was measured and found to be in the order of 90%, so multiple scattering effects were not taken into consideration for the data treatment. For both samples, fixed energy window scans were recorded in the temperature range between −23 and 37 °C in steps of 5 °C to cover both the phase transition from the lamellar gel to the fluid phase at 22 °C and also the transition from the gel to the crystalline phase around 12 °C. Special care was taken for the sample alignment so that the momentum transfer $\hbar\vec{Q}$ at the lipid peak maximum lies in the plane of the membrane bilayers for the parallel orientation. Using Eq. (1), the corresponding angles of 75° and 165° with respect to the incoming beam were calculated for the parallel and perpendicular orientation of the scattering vector toward the membrane surface, respectively,

$$Q = \frac{4\pi}{\lambda}\sin\,\theta. \tag{1}$$

Strictly speaking, the terms "parallel" and "perpendicular" are only true for these particular values; nevertheless, we are using these designations in the course of this paper to distinguish the orientations where these alignments are best visible. Both orientations $\vec{Q}$ parallel and $\vec{Q}$ perpendicular to the membrane surface were measured. We mainly focused on the parallel orientation ($2\theta = 75°$). 3 h per temperature was measured to favor good data statistic collection for this orientation. For the perpendicular orientation, the acquisition time varied between 45 min and 1 h (at higher temperatures in particular). For data correction purposes, an empty cell, a cell with six cleaned wafers, and for normalization a 2 mm vanadium sample were measured. The data evaluation was carried out using the LAMP software available at ILL.[35]

### B. Quasielastic neutron scattering experiments at TOFTOF

QENS experiments have been performed on the same samples at the time-of-flight spectrometer TOFTOF (Ref. 36) at the Munich research reactor FRM II in Garching. Applications of the spectrometer in the field of membrane biophysics can be found in, e.g., Busch *et al.*[37] The incident wavelength was set to $\lambda = 6$ Å, the chopper speed to 12 000 rpm, resulting in an energy resolution of the elastic line of 56 $\mu$eV (FWHM of the elastic line). The setup was chosen in order to compare the results with previous measurements obtained by another group.[13] Both samples were measured in a temperature range from 5 to 25 °C to cover both phase transitions: the pretransition from the $L_\beta$ gel phase to the $P_\beta$ ripple phase at 12 °C as well as the main phase transition from the $P_\beta$ phase to the $L_\alpha$ liquid phase at 22 °C.[11] Spectra were taken every 5 °C. The measuring time per temperature was 5 h. All samples, including a 1.5 mm vanadium sample and a sample holder with six empty wafers and pure $D_2O$ needed for corrections, were measured in one orientation (at 45° with respect to the incident beam) only. In this case $\hbar\vec{Q}$ is mainly parallel to the membrane surface at the alkyl chain correlation peak position ($Q = 1.48\ \text{Å}^{-1}$) for low energy transfers. Earlier QENS experiments on 1,2-dipalmitoyl-*sn*-glycero-3-phosphocholine[13] showed no significant differences in the elastic incoherent structure factor (EISF) for $\hbar\vec{Q}$ oriented parallel and perpendicular to the membrane surface. This fact was confirmed by our elastic data and the QENS data were recorded only for the parallel orientation. From the measured spectra, the scattering of the empty can was subtracted, then they were normalized to vanadium and transformed into (Q,E)-space. The data were binned into 15 groups with $Q$ ranging from 0.44 to 1.56 $\text{Å}^{-1}$. Data reduction was performed with IDA package available onsite,[38] data analysis was done using the PAN package from DAVE software.[39]

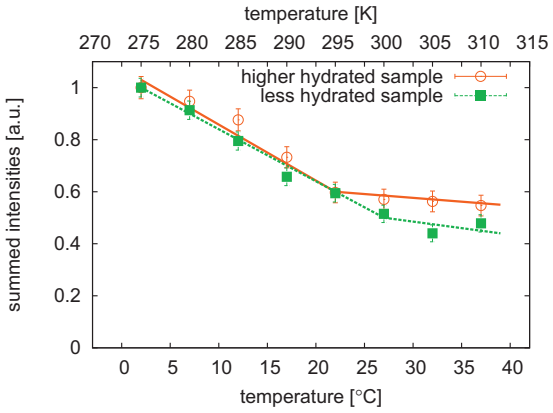


FIG. 2. Plot of the normalized summed elastic intensity vs temperature for $Q$ aligned parallel to the membrane surface. With decreasing water content, a shift in the temperature of the main phase transition is evident. Lines are guides to the eye.

## IV. RESULTS AND DISCUSSION

### A. Elastic data

Figure 2 shows the normalized summed intensity taken on IN13 ($Q$-range: $0.19\ \text{Å}^{-1} < Q < 1.67\ \text{Å}^{-1}$) as a function of temperature for both samples. The representation of the data offers a simple and model-free approach to detect transitions as changes in the elastic intensity decay.[40] In the chosen setup, the influence of the coherent scattering coming from the chain ordering is mainly seen in the parallel orientation. Summed intensities are then shown only for the parallel orientation. The phase transition for the fully hydrated sample is found to lie around 21 °C which coincides very well with the value of 20.15 °C found by Guard-Friar *et al.*[41] Whereas for the less hydrated sample a transition temperature around 25 °C is found. It is known from, e.g., Fourier transform infrared spectroscopy (FTIR) spectroscopy[42] that dehydration increases the transition temperature. Following the procedure used by Pfeiffer *et al.*,[30] we estimated the water content from the shift of the main phase transition temperature. We can extract the parameter $R_w = n_W/n_A$ where $R_w$ expresses the molar ratio of water ($n_W$) and amphiphile ($n_A$).[30,42] The calculated $R_w$ for the fully hydrated sample is $R_w \approx 12$ and $R_w \approx 9$ for the less hydrated sample. Pfeiffer *et al.* found for DMPC multilayers a value of $R_w \approx 12$ for fully

hydrated membranes.[30] Therefore, the elastic measurements on IN13 provide a solid basis to characterize the system for the quasielastic experiment at TOFTOF.

Due to the coherent scattering arising from the ordering of the lipid chains, below the main phase transition and the relatively broad $Q$ resolution of IN13, only three detectors were left to evaluate the mean square displacements (MSDs);[43] therefore, it was not possible to obtain MSDs with reasonable error bars. A detailed comparison between the mean square displacements and the summed intensities for DMPC is found elsewhere.[44]

### B. Quasielastic data

A detailed description of the analysis of quasielastic neutron scattering data can be found in Bée.[45] For applications in the context of lipid dynamics, see, e.g., Busch *et al.*,[37] and for water dynamics in lipid systems, see, e.g., Swenson *et al.*[46]

The obtained data are a convolution of the theoretical scattering law $S_{\text{theo}}(\vec{Q},\omega)$ and the instrumental resolution $S_{\text{res}}(\vec{Q},\omega)$ given by a measured vanadium sample,

$$S_{\text{meas}}(\vec{Q},\omega) = S_{\text{theo}}(\vec{Q},\omega) \otimes S_{\text{res}}(\vec{Q},\omega). \tag{2}$$

The theoretical scattering law can be expressed by a delta function for the elastic contribution and a sum of Lorentzians for the quasielastic contributions coming from the dynamics of the investigated sample.[45] In our study, an elastic peak and two Lorentzian functions (narrow and broad components) were necessary to reasonably fit the obtained data. In Fig. 3 the fits to the data are shown for two $Q$-values. The $S(\vec{Q},\omega)$ writes

$$S_{\text{theo}}(\vec{Q},\omega) = e^{-\text{DWF}}(A_0(\vec{Q})\delta(\omega) + A_1(\vec{Q})L_1(\Gamma_1,\omega) + A_2(\vec{Q})L_2(\Gamma_2,\omega)). \tag{3}$$

$e^{-\text{DWF}}$ is the Debye–Waller factor according for vibrational motions, $\Gamma_i$ represents the half width at half maximum of each Lorentzian, $A_i$ is the corresponding amplitude with the normalization $A_0+A_1+A_2=1$. Keeping in mind that chain-deuterated lipids were used in our experiments, the narrow and the broad Lorentzians were associated with slow and fast motions of the head groups, respectively. The geometry of the motion can be extracted from the EISF as defined in

$$\text{EISF}(\vec{Q}) = \frac{A_0(\vec{Q})}{A_0(\vec{Q}) + A_1(\vec{Q}) + A_2(\vec{Q})}. \tag{4}$$

For both samples, the EISF does not decay to zero for large $Q$-values, which indicates an immobile fraction in the examined time-space window.

Two different models were applied to fit the EISFs. First, we used the "diffusion in a sphere" model introduced by Volino and Dianoux,[47] where free diffusion in the restricted volume of a sphere is permitted. Bellissent-Funel and co-workers[48] established as an addition to this model an immobile fraction. The corresponding EISF is described by

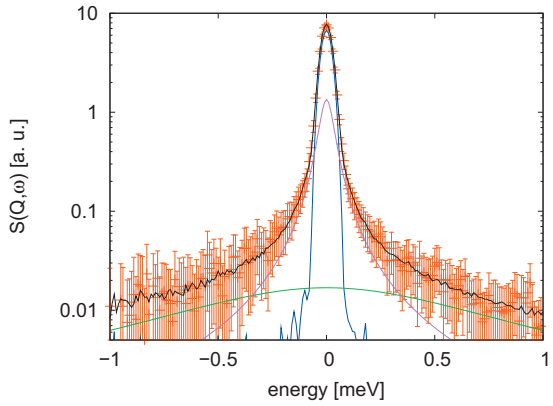


(a)

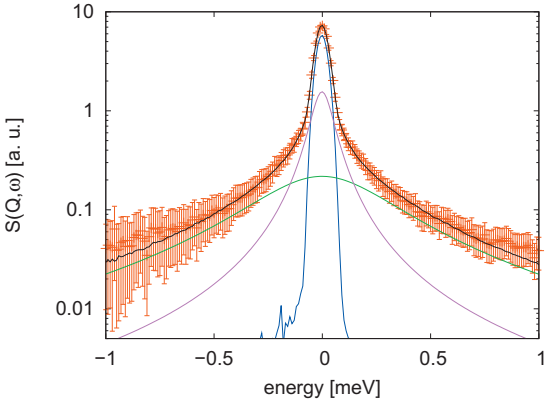


(b)

FIG. 3. Plot of $S(\vec{Q},\omega)$ for (a) $Q$=0.44 Å$^{-1}$ and (b) $Q$=1.48 Å$^{-1}$ at 5 °C. The resulting fit is shown (black line) as well as the single contributions. The delta function is drawn in the blue line; the two Lorentzians are plotted as green and pink lines, respectively.

$$A_0(\vec{Q}) = p + (1-p) \times \left[\frac{3j_1(Qa)}{Qa}\right]^2, \tag{5}$$

where $j_1$ is the first order spherical Bessel function of the first kind, $a$ is the radius of the sphere, $p$ denotes an immobile contribution, and $(1-p)$ is the corresponding mobile fraction.

A modification of the Volino/Dianoux model allows increasing radii for the diffusion volumes of the hydrogen atoms along the head group [see Eq. (6a)]. This model was introduced by Carpentier *et al.* for the study of dicopper tetrapalmitate[49] and is described by

$$A_0(\vec{Q}) = \frac{1}{N}\sum_{n=1}^{N}\left[\frac{3j_1(QR_n)}{QR_n}\right]^2 \tag{6a}$$

with

$$R_n = \frac{n-1}{N-1} \times [R_N - R_1] + R_1. \tag{6b}$$

$N$ stands for the total number of atoms in the chain to which hydrogen atoms are bound (in the case of this study $N$=3). The index $n$ starts with the carbon atom the closest to the oxygen of the phosphorus group which connects the lipid chains with the head group and ends with the nitrogen of the

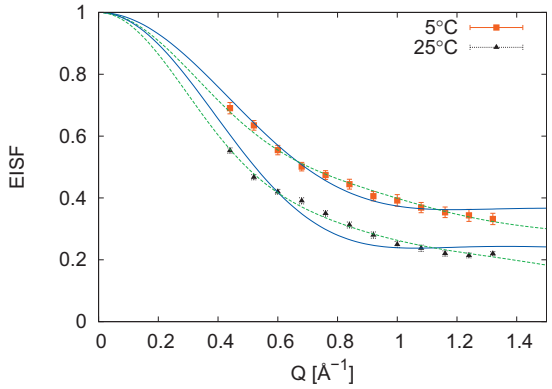


(a)

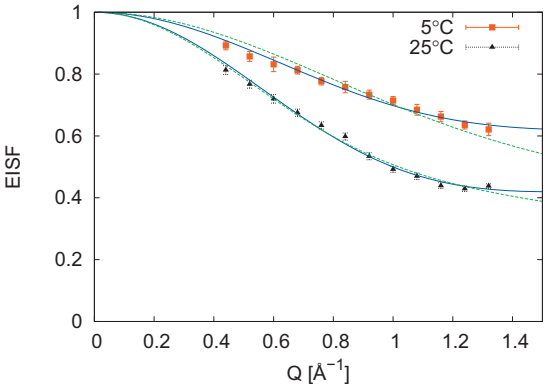


(b)

FIG. 4. EISFs with corresponding fits for the higher hydrated sample (a) and the less hydrated sample (b), respectively. Fits corresponding to the method introduced by Carpentier and co-workers (Ref. 49) are drawn as dashed green lines; fits corresponding to the diffusion in a sphere model (Ref. 47) are drawn as solid blue lines.

choline group (see Fig. 1). $R_n$ gives the radius of the diffusion volume for the corresponding hydrogen atoms. In Eq. (6b) linear increasing radii are assumed. It turned out during the fitting procedure that the choice of $N=3$ yields physically reasonable results, whereas for values bigger than $N=3$ the radius for $R_1$ became negative. Around 1.48 Å$^{-1}$, the coherent scattering rising from the ordering of the lipid chains, the so-called chain correlation peak, is clearly visible. To exclude its influence on the EISF fits, the fit range was restricted to a range of $0.44\ \text{Å}^{-1} < Q < 1.32\ \text{Å}^{-1}$. Figures 4(a) and 4(b) show the obtained data for two temperatures, one below (5 °C) and one above (25 °C), the main phase transition for the fully hydrated sample and the less hydrated sample, respectively. Fits corresponding to the diffusion in a sphere model are shown as solid blue lines, the Carpentier model as dashed green lines. In the case of the less hydrated sample, the diffusion in a sphere model fits the data sufficiently well within the experimental errors, leading to values of $a=2.64(10)$ Å and $a=2.91(06)$ Å for the radii at 5 and 25 °C, respectively. For the higher hydrated sample, the simple model of diffusive motion in a sphere is not longer sufficient. Here, the Carpentier model gives definitely better results, especially at higher temperatures. In the $L_\beta$ gel phase at 5 °C, the fits result in values of $R_{\min}=0.36(4)$ Å for the

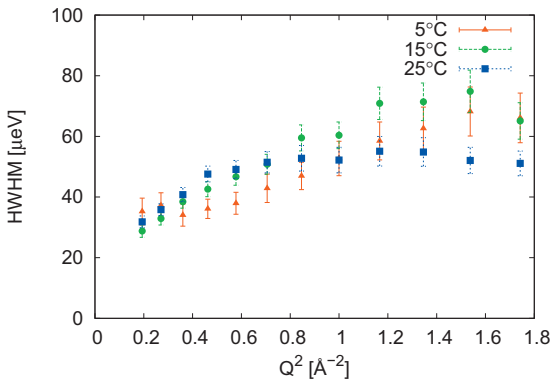


FIG. 5. Line widths for selected temperatures (5, 15, and 25 °C) for the higher hydrated sample.

displacement of the proton bound in the methylene groups near the phosphorus atoms of the lipid and of $R_{\max}=5.05(6)$ Å for the hydrogens of the methyl groups in the choline group. At 25 °C in the liquid $L_\alpha$, phase corresponding values of $R_{\min}=1.14(3)$ Å and $R_{\max}=6.42(11)$ Å were obtained. The fact that the EISF is not going to zero for large $Q$-values is an indication that not all of the protons take part in the movements observed in the chosen time-space window of the experiment, as it has been seen, e.g., for protein-membrane complexes.[50,51] However, for a detailed investigation, a broader $Q$-range would be preferable to clearly distinguish trends. In this context, we want to emphasize that both employed models have only two fit parameters, namely, in the case of the diffusion in a sphere model the radius $a$ and the immobile fraction $p$, and in the Carpentier model the first radius $R_1$ and the last radius $R_N$. We tried also to fit other models to the EISF (with more than two fit parameters) which are often used to analyze methyl group reorientation because of the three head group methyl groups. Namely, the threefold jump model[45] and a variant of this model (applied to the methyl reorientation on trimethyloxosulphonium[52]) have also been fitted to the data but they do not sufficiently well fit the experimental data (data not shown).

Our experiments demonstrate nicely the influence of hydration on the mobility of the protons. The difference in the EISF values shows a strong dependence on the level of hydration. For the diffusion in a sphere model the percentage of immobile protons can be inferred directly from the fit parameter $p$ (see formula (5)), in the case of the Carpentier model different radii for the volume of rotation can be extracted. Thus, for the less hydrated sample, the values for 5 °C amount to $p_{5\,^\circ\text{C}}=61.9(14)\%$ and $p_{25\,^\circ\text{C}}=42.0(8)\%$ for 25 °C, respectively. Even if the diffusion in a sphere model cannot be applied to the higher hydrated sample, it is already clear from comparing Figs. 4(a) and 4(b) that the immobile fraction for the latter sample is lower. With the obtained results, we are able to directly associate different models of motions to a given hydration of the lipids.

Figure 5 shows the line widths $\Gamma$ of the narrower Lorentzian as a function of $Q^2$. The line width of the second Lorentzian is about a factor of 10 larger than the narrow one and it shows a $Q$-independent, constant value for $\Gamma$ for both hydrations (data not shown here). For small $Q$-values

($Q \to 0$), the data do not go to zero as for free diffusion, then they increase and asymptotically reach a constant value $\Gamma_\infty$ for large $Q$. A constant value at small $Q$ was assigned by Volino and Dianoux[47] to a confinement effect at large radii. A similar behavior is assumed and has also been observed by Carpentier *et al.*[49]

However, we find a discrete kink only for the lowest measured temperature (red points in Fig. 5). At this temperature, the confinement radius $R_{conf}$ obtained from the crossover of the two regimes at a $Q^2$-value of about 0.55 Å$^{-1}$ following formula (7) was calculated to be 4.2 (4) Å. These values are in between $R_{min}$ and $R_{max}$ obtained from the EISF fits for the corresponding sample at 5 °C and therefore consistent with these values,

$$Q = \frac{\pi}{R_{conf}}. \tag{7}$$

No pronounced plateau is visible for higher temperatures, but a $\Gamma$ which does not decay to zero for small $Q$ values is still an indication for restricted motion as it has also been observed for proteins.[53,54] As we find several radii for the diffusion volumes in the Carpentier model, a superposition of different kinks leads to the observed behavior, especially at high temperatures. At larger $Q$-values, the line width $\Gamma$ follows the "random jump diffusion" model.[55]

As for the EISF also for the line width, the influence of the coherent scattering arising from the chain ordering around $Q = 1.48$ Å$^{-1}$ occurs below the main phase transition, whereas for 25 °C the predicted plateau is observed. Therefore, the data are drawn in the same range as for the EISF.

## V. CONCLUSIONS

In the present study, we have investigated the hydration dependent behavior of model membrane systems above and below the main phase transition of DMPC with a focus on the head group motion. In contrast to existing studies, we took explicitly into account the hydration effect on the dynamics of model membrane systems. Therefore, we were able to directly associate different models for the motions of the hydrogen atoms in the head group to different hydration levels. The elastic temperature scans show a strong dependence on the hydration: the phase transition temperature is lower (related to a higher mobility of the head groups) in the $L_\alpha$ phase at full hydration compared to the less hydrated sample. The type of head group motions possible in the different samples has been probed in more detail by the performed QENS studies. Here, the hydration influence in the observed time and space window is clearly translated by the different models necessary to fit the obtained elastic incoherent structure factor for the different hydrations and the resulting radii. In summary, this study has shown that hydration of lipid bilayers plays a major role in understanding the dynamics of these kinds of systems and should always be properly characterized when dealing with samples containing lipids.

## ACKNOWLEDGMENTS

The authors thank F. Natali and S. Busch for the fruitful discussions. M. Trapp was supported by a Ph.D. scholarship from the French Ministry for Research and Technology. This research project has been supported by the European Commission under the Sixth Framework Program through the Key Action: Strengthening the European Research Area, Research Infrastructures (Contract No. RII3-CT-2003-5059825). We acknowledge the ILL and the FRM II for the allocation of beamtime and the financial support from the Access to Major Research Facilities Program which is a component of the International Science Linkages Program established under the Australian Government's innovation statement, Backing Australia's Ability.

[1] J. Fitter, S. A. W. Verclas, R. E. Lechner, H. Seelert, and N. A. Dencher, FEBS Lett. **433**, 321 (1998).
[2] J. Zanotti, M.-C. Bellissent-Funel, and J. Parello, Biophys. J. **76**, 2390 (1999).
[3] F. Gabel, D. Bicout, U. Lehnert, M. Tehei, M. Weik, and G. Zaccai, Q. Rev. Biophys. **35**, 327 (2002).
[4] J. Roh, J. Curtis, S. Azzam, V. Novikov, I. Peral, Z. Chowdhuri, R. Gregory, and A. Sokolov, Biophys. J. **91**, 2573 (2006).
[5] J. Pieper, T. Hauß, A. Buchsteiner, and G. Renger, Eur. Biophys. J. **37**, 657 (2008).
[6] K. Wood, U. Lehnert, B. Kessler, G. Zaccai, and D. Oesterhelt, Biophys. J. **95**, 194 (2008).
[7] P. J. Steinbach and B. Brooks, Proc. Natl. Acad. Sci. U.S.A. **90**, 9135 (1993).
[8] M. Tarek and D. J. Tobias, Phys. Rev. Lett. **88**, 138101 (2002).
[9] C.-J. Högberg and A. P. Lyubartsev, J. Phys. Chem. B **110**, 14326 (2006).
[10] T. Heimburg, *Thermal Biophysics of Membranes* (Wiley-VCH, Weinheim, Germany, 2007).
[11] G. S. Smith, E. B. Sirota, C. R. Safinya, and N. A. Clark, Phys. Rev. Lett. **60**, 813 (1988).
[12] W. Pfeiffer, T. Henkel, E. Sackmann, W. Knoll, and D. Richter EPL **8**, 201 (1989).
[13] S. König, W. Pfeiffer, T. Bayerl, D. Richter, and E. Sackmann, J. Phys. II (France) **2**, 1589 (1992).
[14] S. König, T. M. Bayerl, G. Coddens, D. Richter, and E. Sackmann, Biophys. J. **68**, 1871 (1995).
[15] M. Rheinstädter, J. Das, E. Flenner, B. Brüning, T. Seydel, and I. Kosztin, Phys. Rev. Lett. **101**, 248106 (2008).
[16] *Structure and Dynamics of Membranes*, Handbook of Biological Physics Vol. 1, edited by R. Lipowsky and E. Sackmann (Elsevier, Amsterdam, The Netherlands, 1995).
[17] M. C. Rheinstädter, C. Ollinger, G. Fragneto, F. Demmel, and T. Salditt, Phys. Rev. Lett. **93**, 108107 (2004).
[18] M. C. Rheinstädter, W. Häußler, and T. Salditt, Phys. Rev. Lett. **97**, 048103 (2006).
[19] A. A. Nevzorov and M. F. Brown, J. Chem. Phys. **107**, 10288 (1997).
[20] S. König, E. Sackmann, D. Richter, R. Zorn, C. Carlile, and T. M. Bayerl, J. Chem. Phys. **100**, 3307 (1994).
[21] S. H. Chen, C. Y. Liao, H. W. Huang, T. M. Weiss, M.-C. Bellisent-Funel, and F. Sette, Phys. Rev. Lett. **86**, 740 (2001).
[22] B. Klösgen, C. Reichle, S. Kohlsmann, and K. Kramer, Biophys. J. **71**, 3251 (1996).
[23] E. Y. Shalaev and P. L. Steponkus, J. Phys. Chem. B **107**, 8734 (2003).
[24] R. Hirn, T. M. Bayerl, J. O. Rädler, and E. Sackmann, Faraday Discuss. **111**, 17 (1999).
[25] C. Eggeling, C. Ringemann, R. Medda, G. Schwarzmann, K. Sandhoff, S. Polyakova, V. Belov, B. Hein, C. von Middendorff, A. Schonle, and S. Hell, Nature (London) **457**, 1159 (2009).
[26] M. Doxastakis, V. G. Sakai, S. Ohtake, J. K. Maranas, and J. J. de Pablo, Biophys. J. **92**, 147 (2007).
[27] U. Lehnert, V. Réat, M. Weik, G. Zaccaï, and C. Pfister, Biophys. J. **75**, 1945 (1998).
[28] V. F. Sears, Neutron News **3**, 26 (1992).
[29] L. Ding, T. Weiss, G. Fragneto, W. Liu, L. Yang, and H. Huang, Langmuir **21**, 203 (2005).
[30] H. Pfeiffer, H. Binder, G. Klose, and K. Heremans, BBA-Biomembranes **1609**, 148 (2003).
[31] See http://www.ill.eu/d16/.

[32] See supplementary material at http://dx.doi.org/10.1063/1.3495973 for the diffraction data taken on D16 to evaluate the repeat distance and mosaicity of the aligned multilayer samples.
[33] N. Kucerka, Y. Liu, N. Chu, H. I. Petrache, S. Tristram-Nagle, and J. F. Nagle, Biophys. J. **88**, 2626 (2005).
[34] F. Natali, J. Peters, D. Russo, S. Barbieri, C. Chiapponi, A. Cupane, A. Deriu, M. T. Di Bari, E. Farhi, Y. Gerelli, P. Mariani, A. Paciaroni, C. Rivasseau, G. Schiró, and F. Sonvico, Neutron News **19**, 14 (2008).
[35] See http://www.ill.eu/instruments-support/computing-for-science/cs-software/all-software/lamp/.
[36] T. Unruh, J. Neuhaus, and W. Petry, Nucl. Instrum. Methods Phys. Res. A **580**, 1414 (2007).
[37] S. Busch, C. Smuda, L. C. Pardo, and T. Unruh, J. Am. Chem. Soc. **132**, 3232 (2010).
[38] See http://sourceforge.net/projects/frida/.
[39] See http://www.ncnr.nist.gov/dave.
[40] B. Frick and L. J. Fetters, Macromolecules **27**, 974 (1994).
[41] D. Guard-Friar, C. H. Chen, and A. S. Engle, J. Phys. Chem. **89**, 1810 (1985).
[42] H. Pfeiffer, H. Binder, G. Klose, and K. Heremans, BBA-Biomembranes **1609**, 144 (2003).
[43] J. C. Smith, Q. Rev. Biophys. **24**, 227 (1991).
[44] M. Trapp, F. Juranyi, M. Tehei, L. van Eijck, B. Demé, T. Gutberlet, and J. Peters, Spectroscopy **24**, 461 (2010).
[45] M. Bée, *Quasielastic Neutron Scattering: Principles and Applications in Solid State Chemistry, Biology and Materials Science* (Adam Hilger, Philadelphia, 1988).
[46] J. Swenson, F. Kargl, P. Berntsen, and C. Svanberg, J. Chem. Phys. **129**, 045101 (2008).
[47] F. Volino and A. J. Dianoux, Mol. Phys. **41**, 271 (1980).
[48] M.-C. Bellissent-Funel, J. Teixeira, K. Bradley, and S. H. Chen, J. Phys. I (France) **2**, 995 (1992).
[49] L. Carpentier, M. Bée, A. M. Giroud-Godquin, P. Maldivi, and J. C. Marchon, Mol. Phys. **68**, 1367 (1989).
[50] F. Natali, A. Relini, A. Gliozzi, R. Rolandi, P. Cavatorta, A. Deriu, A. Fasano, and P. Riccio, Chem. Phys. **292**, 455 (2003).
[51] F. Natali, A. Relini, A. Gliozzi, R. Rolandi, P. Cavatorta, A. Deriu, A. Fasano, and P. Riccio, Physica B **350**, E623 (2004).
[52] M. Bée, H. Jobic, and C. Sourisseau, J. Phys. C **18**, 5771 (1985).
[53] M. Tehei, J. Smith, C. Monk, J. Ollivier, M. Oettl, V. Kurkal, J. Finney, and R. Daniel, Biophys. J. **90**, 1090 (2006).
[54] Z. Bu, D. A. Neumann, S.-H. Lee, C. M. Brown, D. M. Engelman, and C. C. Han, J. Mol. Biol. **301**, 525 (2000).
[55] P. A. Egelstaff, *An Introduction to the Liquid State* (Academic Press, New York, 1967).